Conical Flow near External Axial Corners as a Bifurcation Problem

Peter G. Bakker* and John W. Reyn†
Delft University of Technology, Delft, the Netherlands

The supersonic flow around configurations consisting of two plane delta wings, attached to each other along a common edge, forming an external corner is discussed on the basis of potential conical flow theory. The occurrence and character of conical stagnation points are studied as a bifurcation from the starlike node in the conical streamline pattern, which occurs at the corner point in a uniform flow. Various bifurcation modes are possible, including those where nodal points move away from the corner on which a saddle point is formed. As an example, the flow around a symmetrical external corner is discussed to illustrate the use of the first bifurcation mode to obtain a better understanding of the flowfield. As a result, the flow pattern with a saddle point at the corner flanked by two nodal points on the body surface is confirmed. Comparison is made with numerical calculations and experimental results.

Introduction

IN this paper the authors discuss the supersonic flow around configurations consisting of two plane delta wings Σ_1 and Σ_2 attached to each other along a common edge, such that the planes of the wings make an angle with each other. The two remaining free (leading) edges are supersonic; thus the flows on either side of the configuration can be considered independently. Furthermore, the flow will be assumed to be conical, and with the center of the conical field coinciding with the apex of the configuration. The authors will be concerned with the flow in the region of the external angle of the configuration, including both the case of the external axial corner, wherein the plane wings are nearly perpendicular to each other, and the case wherein the configuration is similar to one side (upper or lower) of a delta wing with rhombic cross section.

In order to describe the configuration in more detail, let us introduce a right-handed Cartesian coordinate system x_1,y_1z_1, with the origin in the apex of the configuration and the positive x_1 axis directed along the direction of the undisturbed stream, as indicated in Fig. 1. The y_1 axis is chosen such that the leading edge of wing Σ_1 is in the x_1y_1 plane, and the z_1 axis is perpendicular to the x_1y_1 plane. The leading edge of Σ_1 has a sweep angle Λ_1 at the y_1 axis and Σ_1 is inclined with respect to the x_1y_1 plane at an angle δ_1, measured in the x_1z_1 plane. The leading edge of wing Σ_2 and the x_1 axis determine a plane Ω, which makes an angle ω with the x_1y_1 plane measured positive, as indicated in Fig. 1. The leading edge of Σ_2 has a sweep angle Λ_2 with the y_1z_1 plane and Σ_2 makes an angle δ_2 with Ω, where δ_2 is measured in a plane through the x_1 axis and perpendicular to the plane Ω. The line where wings Σ_1 and Σ_2 meet each other will be called the corner line.

The conical symmetry of the flowfield allows the flow to be described by the variables $\eta_1=y_1/x_1$ and $\zeta_1=z_1/x_1$. These variables may be visualized in a plane normal to the undisturbed stream at unit distance downstream of the apex. The intersection lines of Σ_1 and Σ_2 with this plane are indicated by s_1 and s_2, respectively, and the intersection point with the corner line by C (corner point).

Received Aug. 15, 1983; revision received March 25, 1984.

*Senior Research Scientist, Department of Aerospace Engineering.
†Professor, Department of Mathematics.

The supersonic flow around an external corner was investigated by several authors.[1-6] The occurrence and character of conical stagnation points in this flow pattern in relation to the flow near the corner point has received particular attention. In the symmetrical case ($\Lambda_1=\Lambda_2$, $\delta_1=\delta_2$), the corner point is a conical stagnation point; in the asymmetrical case, the possibility that the flow will spill over the corner to the low-pressure side and a conical Prandtl-Meyer fan will be formed at the corner point must be considered as well.[2,4] The study will be restricted to the case wherein the corner point is a conical stagnation point. If the boundary conditions on the wing surfaces are taken into account in local conical stagnation point solutions, various possibilities for the type of conical stagnation points at the corner arise, such as an oblique saddle point or a starlike node. In numerical calculations made by Kutler and Shankar[3] for both symmetrical ($\Lambda_1=\Lambda_2=0$, $\delta_1=\delta_2=10$ deg, $\omega=90$ deg) and asymmetrical configurations ($\Lambda_1=-30$ deg, -30 deg$<\Lambda_2<30$ deg, $\delta_1=\delta_2=0$ deg, $\omega=90$ deg), an oblique saddle point in the conical streamline pattern was found at the corner point, and a nodal point on each of the wing surfaces; the position of this point corresponds to the point where the transverse pressure distribution over the wing surface attains a minimum. A qualitative sketch of this flow pattern is given in Fig. 2a. The same flow pattern was also found in experiments[1,2] made for $M_\infty=2.95$, $\Lambda_1=\Lambda_2=0$, $\delta_1=\delta_2=10.3$

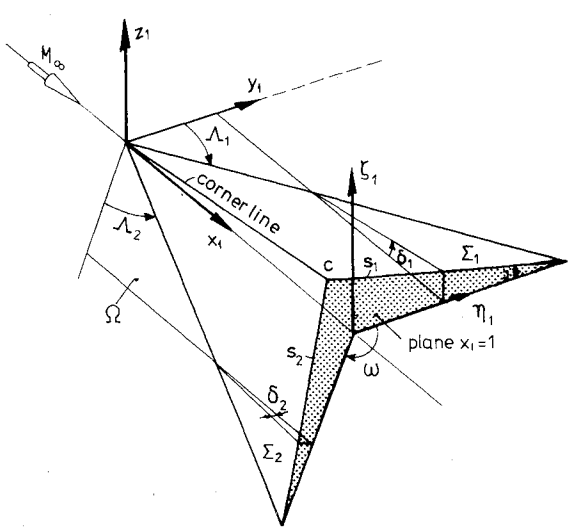

Fig. 1 Coordinate system and geometry of the external axial corner.

deg for the symmetrical case. Despite this numerical and experimental evidence, a flow pattern, as sketched in Fig. 2b, having a nodal point in the corner point as the only conical stagnation point in the flowfield, should also be considered.[4] In fact, a numerical study by Salas[5] for symmetrical configurations with $\Lambda_1=\Lambda_2=20$ deg, $\delta_1=\delta_2=10$ deg and a variation of the angle ω from $\pi/2$, representing the corner type, to π, representing the delta wing type, seems to indicate the occurrence of the flow pattern of Fig. 2b for angles ω close to π. Also, the calculations suggest a transition from the pattern given in Fig. 2a to that given in Fig. 2b if ω is varied from $\pi/2$ to π. It is one of the aims of the present paper to investigate whether local solutions of the potential flow in the vicinity of conical stagnation points at the corner support this second type of flow and the possibility of transition from the first flow pattern to the second pattern at some critical value of ω.

The real nature of the conical stagnation point in the flow under discussion can be found only by solving the full nonlinear boundary value problem, without using approximations such as numerical solutions. This, of course, is a difficult problem, unlikely to be solved. However, there is one notable exception, namely, if $\delta_1=\delta_2=0$, in which case Σ_1 and Σ_2 are aligned with the uniform flow. The resulting flow is the undisturbed uniform flow and the conical streamline pattern contains a single starlike node at the corner point. In the present paper we will consider the local corner flow as a perturbation of this flow and the conical stagnation points at and near the corner point as bifurcations of this starlike node. Within the class of potential flows near a conical stagnation point, only those perturbed flows will be admitted which satisfy the boundary condition on the surfaces Σ_1 and Σ_2, and which revert to the uniform flow with the starlike node at the corner point if $\delta_1, \delta_2 \to 0$.

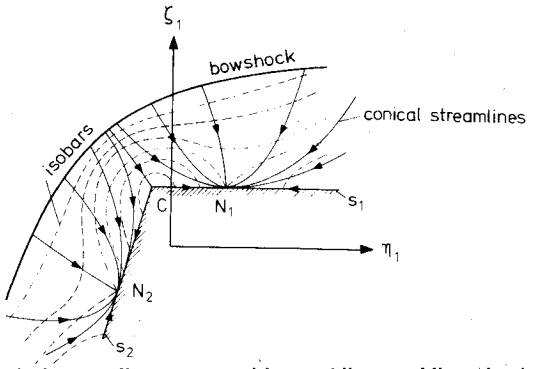

a) Conical streamline pattern with an oblique saddle point in the corner point (C) and two nodal points (N_1 and N_2).

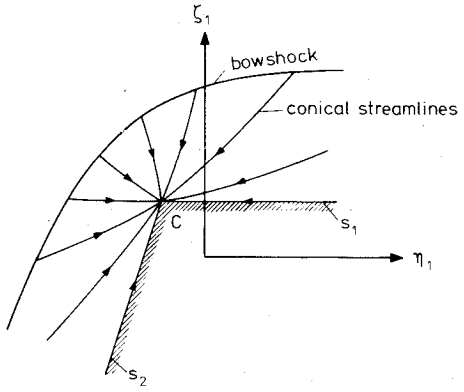

b) Conical streamline pattern with a single node at the corner point.

Fig. 2 Possible conical flow patterns near the corner point of an external corner.

Potential Flow Solutions near Conical Stagnation Points

Potential flow solutions near conical stagnation points were given in Ref. 1, from which now, with slight modifications, some results will be listed, which will be used in the following. The flow was analyzed in a plane normal to the radius through the conical stagnation points (on this radius the velocity vector is radial). Correspondingly, the flow around the corner will be investigated in a plane normal to the corner line; such a plane will be called a cross-flow plane. At variance with the coordinate system introduced before, we now use a right-handed coordinate system x,y,z where the positive x axis coincides with the corner line and the y axis lies in the Σ_1 plane, any plane parallel to the yz plane being a cross-flow plane. The largest angle between planes Σ_1 and Σ_2 will be indicated by Φ_e (external angle) and determined from the parameters δ_1, δ_2, Λ_1, Λ_2, and ω. For small inclinations of the corner line with respect to the oncoming flow, the two coordinate systems do not differ much.

We assume an inviscid, non-heat-conducting, perfect gas with ratio of specific heats $\gamma=C_p/C_v$. The flow is assumed to be irrotational so that a velocity potential $\Phi=\Phi(x,y,z)$ may be introduced such that $\nabla\Phi=q=(u,v,w)$, where u,v,w denote the components of the velocity q along x,y,z axes, respectively. Since the flow is conical $\Phi=x\cdot F(\eta,\zeta)$ may be written where F is the conical potential and $\eta=y/x$, $\zeta=z/x$ are the variables y and z in the cross-flow plane at $x=1$.

The conical streamlines in the cross-flow plane will be obtained by integration of the velocity vector field in that plane $(v-u\eta,\ w-u\zeta)$ which yields the equations for the conical streamlines

$$\frac{d\eta}{dt}=v-u\eta, \qquad \frac{d\zeta}{dt}=w-u\zeta \tag{1}$$

In this paper it is convenient to work with polar coordinates in the cross-flow plane $\eta=\rho\cos\varphi$, $\zeta=\rho\sin\varphi$, $0\le\varphi<2\pi$, $\rho\ge 0$; then the velocity components may be written

$$u=F-\rho F_\rho, \quad v=F_\rho\cos\varphi-\frac{1}{\rho}F_\varphi\sin\varphi, \quad w=F_\rho\sin\varphi+\frac{1}{\rho}F_\varphi\cos\varphi \tag{2}$$

The conical potential F obeys the following second-order nonlinear differential equation

$$[a^2(1+\rho^2)-\{\rho F-(1+\rho^2)F_\rho\}^2]F_{\rho\rho}+2\left\{F-\left(\rho+\frac{1}{\rho}\right)F_\rho\right\}\times\left(\frac{1}{\rho}F_{\rho\varphi}-\frac{1}{\rho^2}F_\varphi\right)F_\varphi+\left(a^2-\frac{1}{\rho^2}F_\varphi^2\right)\left(\frac{1}{\rho^2}F_{\varphi\varphi}+\frac{1}{\rho}F_\rho\right)=0 \tag{3}$$

where a is the local speed of sound related to the speed $|q|$ by

$$a^2=\frac{\gamma-1}{2}(1-|q|^2) \tag{4}$$

and the velocities are nondimensionalized by the maximum speed $q_{\max}$. The conical streamlines are the integral curves of the system

$$\frac{d\rho}{dt}=(1+\rho^2)F_\rho-\rho F, \qquad \frac{d\varphi}{dt}=\frac{F_\varphi}{\rho^2} \tag{5}$$

In Ref. 1, conical stagnation solutions of Eq. (3) were found in the form

$$F=F_0[1+\rho^n F_n(\varphi)+\rho^m F_m(\varphi)+o(\rho^m)], \quad 1<n<m \quad (6)$$

where F_0 is a constant which equals the nondimensionalized radial velocity component in the conical stagnation point. The potential $F(\rho,\varphi)\equiv F_0$ yields a uniform parallel flow with a conical stagnation point at $\rho=0$. If Eq. (6) is substituted into Eq. (5) and the result is ordered with respect to powers in ρ, the following solutions for $F_n(\varphi)$ and $F_m(\varphi)$ are obtained in Ref. 1:

$$F_n(\varphi)=\epsilon_n\cos(n\varphi+\psi_n), \quad n>1 \quad (7)$$

$$F_m(\varphi)=\beta_m\cos(m\varphi+\chi_m), \quad n<m<m_c \quad (8a)$$

$$=\beta_m\cos(m\varphi+\chi_m)+\gamma_m\cos(n\varphi+\psi_n)+\delta_m, \quad m=m_c \quad (8b)$$

The quantities ϵ_n, ψ_n, β_m, and χ_m are arbitrary constants; m_c is the maximum value of m for which $F_m(\varphi)$ exists, satisfying the conditions $m_c=3n-2$ for $1<n\leq 2$ and $m_c=n+2$ if $n\geq 2$. Furthermore, for $1<n<2$: $\gamma_m=n^3M_0^2\epsilon_n^3/(8n-4)$, $\delta_m=0$; for $n=2$: $\gamma_m=(M_0^2-1-4\epsilon_n^2M_0^2)\epsilon_n/6$, $\delta_m=-\epsilon_n^2M_0^2/2$; and for $n>2$: $\gamma_m=n(n-1)(M_0^2-1)\epsilon_n/(2n+4)$, $\delta_m=0$, where M_0 is the local Mach number at the corner point.

With the aid of the listed solutions for the conical velocity potential and Eq. (1) or (5), the conical streamline pattern near the corner point may be determined. The pressure distribution is given by the relation

$$\left(\frac{p}{p_0}\right)^{\frac{\gamma-1}{\gamma}}=\frac{1-(u^2+v^2+w^2)}{1-u_0^2} \quad (9)$$

where the zero subscript indicates conditions in the conical stagnation point.

Boundary Conditions, Bifurcation Modes

The solutions given before describe potential flow patterns near conical stagnation points. For flows with a conical stagnation point at the corner point, the boundary condition $d\varphi/dt=0$ have to be satisfied at $\Sigma_1(\varphi=0)$ and $\Sigma_2(\varphi=\Phi_e)$. Then, with Eq. (6),

$$F_n'=F_m'=0 \text{ at } \varphi=0 \text{ and } \varphi=\Phi_e \quad (10)$$

where primes denote differentiation with respect to φ. Application of these conditions to the solutions given before yields

$$\psi_n=\chi_m=0 \quad (11a)$$

and

$$n=k(\pi/\Phi_e), \quad k=2,3,4,\ldots$$

$$m=\ell(\pi/\Phi_e), \quad \ell=3,4,5,\ldots$$

or

$$m=m_c\neq\ell(\pi/\Phi_e), \quad \beta_m=0 \quad (11b)$$

Since external corner flows are considered with an external angle $\pi\leq\Phi_e\leq 2\pi$ and $m>n>1$, it follows that $\ell>k\geq 2$.

Obviously, imposing the boundary conditions on Σ_1 and Σ_2 is, by itself, insufficient to ensure the proper embedding of the conical stagnation point solution near the corner in a given surrounding main flow. In fact, the freedom to further specify solutions is already expressed by the possiblity of choosing the values of k and ℓ in the leading terms of the expansion for the conical potential. The exponent n, occurring in the leading term, is illustrated in Fig. 3 as a function of the external angle Φ_e for various values of k.

The properties of the solutions for the various choices of k and ℓ will now be investigated. These solutions will be considered as perturbations of the uniform flow, given by $F=F_0$ and having a conical streamline pattern with a starlike node at the corner point [Eq. (5)]. Therefore, the coefficients in the expansion for the conical potential [Eq. (6)], such as ϵ_n, β_m, etc., will be interpreted as small parameters tending to zero to obtain the uniform flow. These small parameters vary in relation to each other such that $\rho^nF_n(\varphi)$ remains the leading term in the expansion, even if they tend to zero. In general, the perturbation of the uniform flow will result in a change of the conical streamline pattern. This will be called a bifurcation phenomenon if a topologically different structure of this pattern is obtained, involving the generation of new conical stagnation points. These new stagnation points will be considered as results of bifurcation of the original starlike node at the corner point. The various bifurcation modes of the starlike node are characterized by giving the value of k.

Bifurcations of the Starlike Node

First Bifurcation Mode ($k=2$, $n=2\pi/\Phi_e$)

In the first bifurcation mode, $k=2$, the exponent n occurring in the leading term of Eq. (6) can take the values $1<n\leq 2$ corresponding to external angles $\pi\leq\Phi_e<2\pi$; the external angle $\Phi_e=2\pi$ must be excluded because a conical stagnation point requires $n>1$. From Eq. (11b) it follows that $m=m_c=3n-2$ if $1<n\leq 4/3$ and $m=3n/2$ if $4/3\leq n\leq 2$. The conical streamline pattern near the corner point may be obtained from Eq. (5), leading to the following expressions:

$$\frac{d\rho}{dt}=F_0\{n\epsilon_n\rho^{n-1}\cos(n\varphi)+\mathcal{O}(\rho^{m-1})-\rho\}$$

$$\rho\frac{d\varphi}{dt}=F_0\{-n\epsilon_n\rho^{n-1}\sin(n\varphi)+\mathcal{O}(\rho^{m-1})\} \quad (12)$$

In conical stagnation points the conditions $d\rho/dt=d\varphi/dt=0$ have to be satisfied.

For $1<n<2$ it follows from Eq. (12) that for small values of ϵ_n, β_m, etc., as locations of the conical stagnation points.

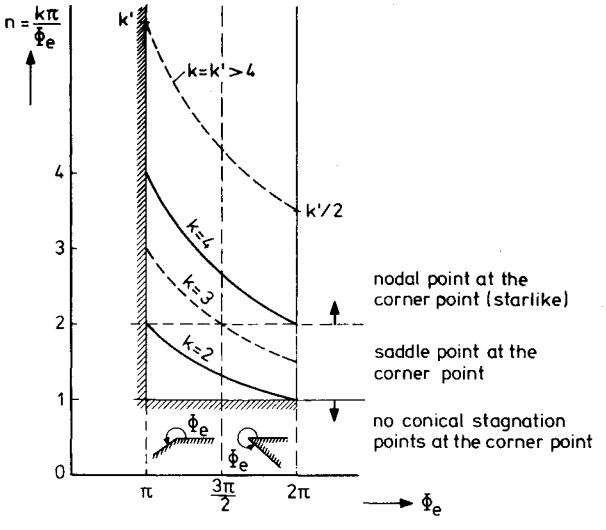

Fig. 3 Dependance of n on the external angle for different bifurcation modes. $k=2$ first bifurcation mode, $k=3$ second bifurcation mode, $k=4$ third bifurcation mode, and $k=k'(k'-1)$ bifurcation mode.

$$C: \quad \rho = 0 \text{ (corner points)}$$

$$N_1, N_2: \quad \varphi_1 = 0,\ \varphi_2 = \Phi_e,\ \rho_1 = \rho_2 = (n\epsilon_n)^{1/(2-n)};\ \epsilon_n > 0$$

$$N_3: \quad \varphi_3 = \frac{\Phi_e}{2},\ \rho_3 = (-n\epsilon_n)^{1/(2-n)};\ \epsilon_n < 0 \tag{13}$$

where higher order terms in ϵ_n and β_m, etc., are omitted. From Eq. (13) it can be seen that, apart from the conical stagnation point at the corner C, there are either two stagnation points N_1 and N_2 located on the surfaces Σ_1 and Σ_2 respectively, or there is one point N_3 which is a free singularity in the flowfield, Fig. 4a. All of these points approach C as $\epsilon_n \to 0$ and may be viewed as bifurcations of the starlike node in the uniform flow.

The character of the conical stagnation points N_1, N_2, and N_3 may be analyzed by the usual method of linearization.[7] It appears that all of these points possess the character of a node. The nodal points, located on the surfaces Σ_1 and Σ_2, have an infinite number of streamlines tangent to these surfaces. The nodal point N_3 is situated, to a first approximation, on the bisector $\varphi = \frac{1}{2}\Phi_e$ in such a way that an infinite number of streamlines is tangent to this bisector. The conical stagnation point C at the corner is an oblique saddle point.[1] The oblique saddle point has three separatrices; two of them coincide with the surfaces Σ_1 and Σ_2, the third with the bisector $\varphi = \frac{1}{2}\Phi_e$.

For $n = 2(\Phi_e = \pi)$, the analysis of the streamline pattern near the corner point is more conveniently performed using the Cartesian coordinates η and ζ. Equation (6) then becomes

$$F = F_0\{1 + \epsilon_n(\eta^2 - \zeta^2) + \mathcal{O}(\rho^3)\} \tag{14}$$

Substitution of Eq. (14) into Eq. (1) leads to the following expression for the conical streamlines:

$$\frac{d\eta}{dt} = F_0(2\epsilon_n - 1)\eta + \mathcal{O}(\rho^2)$$

$$\frac{d\zeta}{dt} = -F_0(2\epsilon_n + 1)\zeta + \mathcal{O}(\rho^2) \tag{15}$$

In contrast to the case $1 < n < 2$ we observe that for $n = 2$ there are no conical stagnation points which approach to $\eta = \zeta = 0$ when $\epsilon_n \to 0$ and $\eta = \zeta = 0$ is the conical stagnation point. For $\epsilon_n = 0$ point $C(0,0)$ is the starlike node of the uniform flow. For small values of ϵ_n ($\epsilon_n < \frac{1}{2}$) a nodal point is formed at C such that an infinite number of streamlines is tangent to the η axis for $\epsilon_n > 0$ and to the ζ axis for $\epsilon_n < 0$, Fig. 4b.

Second Bifurcation Mode ($k = 3$, $n = 3\pi/\Phi$)

In the second bifurcation mode $k = 3$, the exponent n occuring in the leading term of Eq. (6) can take the values $3/2 \le n \le 3$ corresponding to external angles $\pi \le \Phi_e \le 2\pi$. This possible range of n, together with the boundary conditions [Eq. (11)], shows that m satisfies the inequality $m \ge 4n/3$.

Substitution of Eq. (6) into Eq. (5) leads to the following expression for the conical streamlines:

$$\frac{d\rho}{dt} = F_0(n\epsilon_n\rho^{n-1}\cos(n\varphi) - \rho + \mathcal{O}(\rho^{4n/3-1}))$$

$$\rho\frac{d\varphi}{dt} = F_0(-n\epsilon_n\rho^{n-1}\sin(n\varphi) + \mathcal{O}(\rho^{4n/3-1})) \tag{16}$$

For $3/2 \le n < 2$, the following conical stagnation points can appear in the neighborhood of the conical stagnation in C:

$$C: \quad k = 0 \text{ (corner point)}$$

$$N_1, N_3: \quad \varphi_1 = 0,\ \varphi_3 = \tfrac{2}{3}\Phi_e,\ \rho_1 = \rho_3 = (n\epsilon_n)^{1/(2-n)};\ \epsilon_n > 0$$

$$N_2, N_4: \quad \varphi_2 = \tfrac{1}{3}\Phi_e,\ \varphi_4 = \Phi_e,\ \rho_2 = \rho_4 = (-n\epsilon_n)^{1/(2-n)};\ \epsilon_n < 0 \tag{17}$$

where higher order terms in ϵ_n, β_m, etc., are omitted.

From Eq. (17) it follows that the second bifurcation mode has in common with the first bifurcation mode that new conical stagnation points are generated from the original starlike node. The points N_1 and N_4 are located on the surfaces Σ_1 and Σ_2, respectively, whereas the points N_2 and N_3 appear as free singularities in the flowfield, see Fig. 5a. For $\epsilon_n > 0$ only the points C, N_1, and N_3 exist and for $\epsilon_n < 0$ the

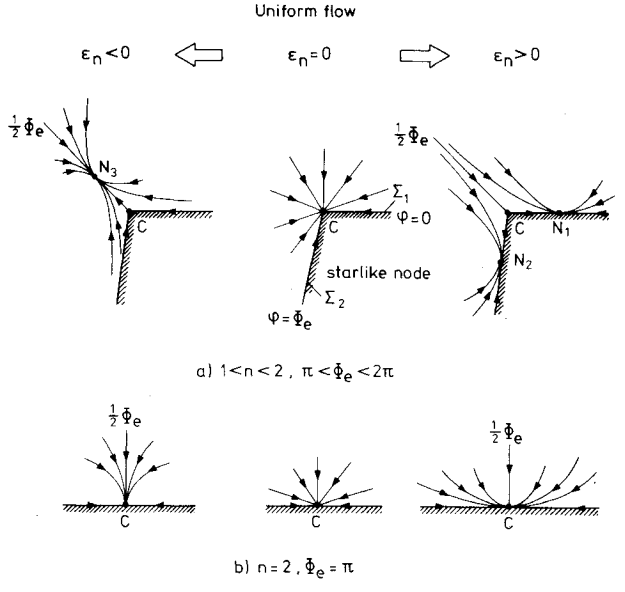

Fig. 4 First bifurcation mode of the starlike node ($k = 2$).

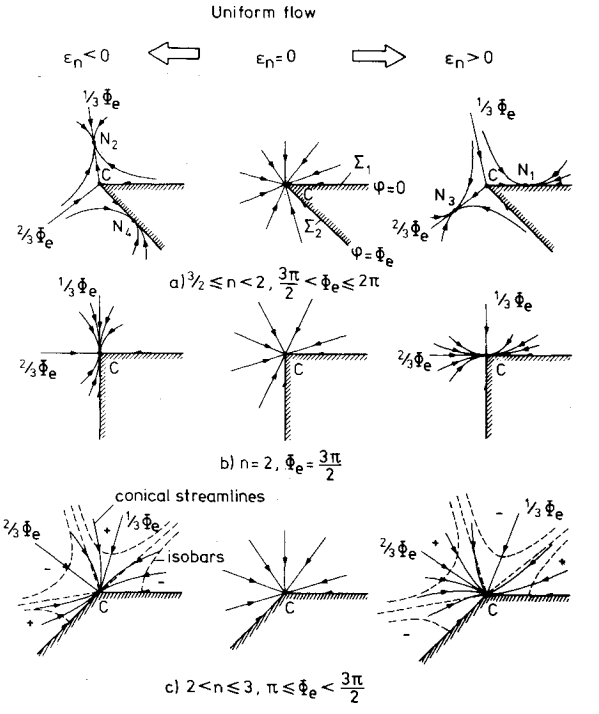

Fig. 5 Second bifurcation mode of starlike node ($k = 3$).

points C, N_2, and N_4 are present. The method of linearization[7] shows that points N_1,N_2,N_3,N_4 are nodal points. The nodal points N_1 and N_4 have an infinite number of streamlines tangent to the surface. The nodal points N_2 and N_3 are situated on the separatrices $\varphi=\frac{1}{3}\Phi_e$ and $\frac{2}{3}\Phi_e$ such that an infinite number of streamlines are tangent to the separatrix. The conical stagnation point C is an oblique saddle point with four separatrices; two of them coincide with the surfaces Σ_1 and Σ_2, whereas the others tend to C along $\varphi=\frac{1}{3}\Phi_e$ and $\frac{2}{3}\Phi_e$, respectively. It is concluded that in the second bifurcation mode for $3/2\leq n<2$ a starlike node bifurcates into an oblique saddle point at the corner point flanked by two nodes. One of these nodes lies on one of the surfaces (Σ_1 or Σ_2), whereas the second node appears as a free singularity in the flow.

The case $n=2$ corresponds to an external angle $\Phi_e=3/2\pi$ and for the conical streamline pattern near the corner Eq. (15) may be used again. In contrast to the case $3/2\leq n<2$ it is observed that for $n=2$ there are no conical stagnation points bifurcating from the starlike node at the corner point. For small values of ϵ_n ($\epsilon_n<\frac{1}{2}$) a nodal point is formed at C with an infinite number of streamlines tangent to the η axis for $\epsilon_n>0$ and to the ζ axis for $\epsilon_n<0$, Fig. 5b.

For the case $2<n\leq 3$ the external angle lies in the range $\pi\leq\Phi_e<3/2\pi$. From Eq. (16) it follows that there are no conical stagnation points tending toward the corner point C for $\epsilon_n\to 0$. For $\epsilon_n\neq 0$ the corner point remains a starlike node.[1]

Equation (16) also shows that the rays $\varphi=\frac{1}{3}\Phi_e$ and $\frac{2}{3}\Phi_e$ are to a first approximation conical streamlines which divide the flowfield into three sectors. Again to a first approximation, the conical streamlines in each sector are curved at the singular point, but the sign of the curvature is opposite in adjacent sectors. The corresponding flow patterns are sketched in Fig. 5c. The pressure distribution near the corner, which may be obtained from Eq. (9) is given by

$$\left(\frac{p}{p_0}\right)^{\frac{\gamma-1}{\gamma}}=1-\frac{F_0^2}{1-F_0^2}\{-2(n-1)\epsilon_n\rho^n\cos(n\varphi)$$
$$+n^2\epsilon_n^2\rho^{2n-2}+\mathcal{O}(\rho^{7n/3-2})\} \tag{18}$$

The isobar pattern shows a saddle point behavior[1] with separatrices at $\varphi=1/6\Phi_e$, $3/6\Phi_e$, and $5/6\Phi_e$ on which $p=p_0$.

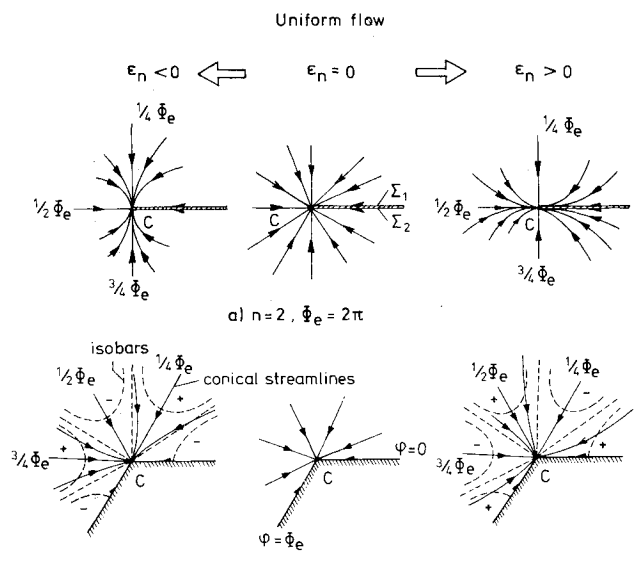

Fig. 6 Third bifurcation mode of starlike node ($k=4$).

It may be noted that in contrast to the first bifurcation mode, the second bifurcation mode is not symmetric with respect to $\varphi=\frac{1}{2}\Phi_e$.

Third Bifurcation Mode ($k=4$, $n=4\pi/\Phi_e$)

In the third bifurcation mode $k=4$, the exponent n occurring in the leading term of Eq. (6) can take the values $2\leq n\leq 4$ corresponding to external angles $\pi\leq\Phi_e\leq 2\pi$. This possible range of n, together with the boundary conditions, Eqs. (11), shows that m satisfies the inequality $m\geq 5n/4$.

Substitution of Eq. (6) into Eq. (5) yields the following expression for the conical streamlines:

$$\frac{d\rho}{dt}=F_0[-\rho+n\epsilon_n\rho^{n-1}\cos(n\varphi)+\mathcal{O}(\rho^{5n/4-1})]$$
$$\rho\frac{d\varphi}{dt}=F_0[-n\epsilon_n\rho^{n-1}\sin(n\varphi)+\mathcal{O}(\rho^{5n/4-1})] \tag{19}$$

This expression reveals that, apart from the conical stagnation point at the corner point C, there are no neighboring conical stagnation points in the flowfield which tend to C for $\epsilon_n\to 0$.

For $n=2$, $\Phi_e=2\pi$ and Eq. (15) may also be used instead of Eq. (19) and a streamline pattern with a single node at the corner point results, Fig. 6a.

For $n>2$, there is a starlike node at the corner point similar to that found in the second bifurcation mode. However, the number of sectors is now four and the rays $\varphi=\frac{1}{4}\Phi_e$, $2/4\Phi_2$, and $\frac{3}{4}\Phi_e$ are the conical streamlines which border these sectors. The corresponding flow patterns that occur in this bifurcation mode are sketched in Fig. 6b.

The pressure distribution near the corner, which may be obtained from Eq. (9), is given by

$$\left(\frac{p}{p_0}\right)^{\frac{\gamma-1}{\gamma}}=1-\frac{F_0^2}{1-F_0^2}\{-2(n-1)\epsilon_n\rho^n\cos(n\varphi)$$
$$+n^2\epsilon_n^2\rho^{2n-2}+\mathcal{O}(\rho^{9n/4-2})\} \tag{20}$$

The isobar pattern shows a saddle point behavior[1] with separatrices at $\varphi=\frac{1}{8}\Phi_e$, $\frac{3}{8}\Phi_e$, $\frac{5}{8}\Phi_e$, and $\frac{7}{8}\Phi_e$ on which $p=p_0$. We note in particular that the pressure on the walls (Σ_1 and Σ_2) and on the bisector $\varphi=\frac{1}{2}\Phi_e$ increases with the distance to the corner point for $\epsilon_n>0$ and decreases for $\epsilon_n<0$, Fig. 6b.

Higher Bifurcation Modes [$k\geq 5$, $n=k(\pi/\Phi_e)$]

For $k\geq 5$ the exponent n satisfies $n>2$ and $\pi\leq\Phi_e\leq 2\pi$. For the conical streamline pattern the leading terms in Eq. (19) may be used again, leading similarly to a starlike node at the corner point, having k sectors. It may be noted that as $k\to\infty$ the flow pattern resembles the uniform flow more and more.

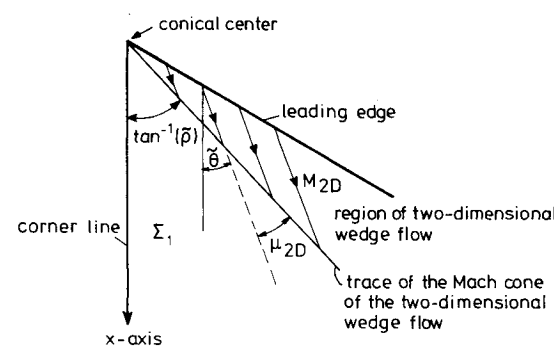

Fig. 7 Matching of local corner flow with two-dimensional wedge flow at the Mach cone.

Symmetrical External Corners

In order to illustrate the use of the classification of bifurcation modes of the starlike node, the flow around a symmetrical external corner will be discussed. The symmetry implies that $k=2,4,6$ and that the generation of conical stagnation points from the starlike node only occurs in the first bifurcation mode ($k=2$). In order to gain more insight into the question whether new conical stagnation points are generated or not, the first mode will be investigated in more detail; in particular the question of how the local corner flow fits within the overall flowfields will be discussed. The pressure distribution on the body surface and the location of the conical stagnation points as a function of freestream Mach number and body geometry will receive special attention. The external angle Φ_e is related to wedge angle δ, sweep angle Λ, and ω by

$$\Phi_e = 2\pi - \cos^{-1}\{[2\tan\delta\tan\Lambda\sin\omega + (1-\tan^2\delta\tan^2\Lambda)\cos\omega - \tan^2\delta]\}/[1+\tan^2\delta+\tan^2\delta\tan^2\Lambda] \tag{21}$$

where $0\le\cos^{-1}\le\pi$, since $\pi\le\Phi_e\le 2\pi$.

For the first bifurcation mode the expansion for the conical potential F may be written as [Eqs. (6), (7), (8b), and (11)]

$$F = F_0(1+\epsilon_n\rho^n\cos(n\varphi)+\lambda\epsilon_n^3\rho^{3n-2}\cos(n\varphi)+o(\rho^{3n-2})) \tag{22}$$

where $\lambda=[n^3M_0^2/4(2n-1)]$, $1<n\le 2$, $\Phi_e=2\pi/n$.

The pressure distribution may be obtained, using Eqs. (2), (9), and (22), as

$$\left(\frac{p}{p_0}\right)^{\frac{\gamma-1}{\gamma}} = 1-\frac{\gamma-1}{2}M_0^2[n^2\epsilon_n^2\rho^{2n-2}-2(n-1)\epsilon_n\rho^n\cos(n\varphi) + 2n\lambda\epsilon_n^4\{n+2(n-1)\cos^2(n\varphi)\}\rho^{4n-4}+o(\rho^{4n-4})] \tag{23}$$

where p_0 and M_0 refer to values in the corner point.

Since we are particularly interested in the flow around an external corner with compressive surfaces ($\delta>0$), and it will be shown later that embedding of the local corner flow is only possible for $\epsilon_n>0$, we will restrict the study to $\epsilon_n>0$ in which case a saddle point occurs at the corner and two nodal points on the body surface at $\rho=\rho_N$. When Eq. (23) is written in terms of ρ_N, using Eq. (13), we obtain

$$\left(\frac{p}{p_0}\right)^{\frac{\gamma-1}{\gamma}} = 1-\frac{\gamma-1}{2}M_0^2\left\{\rho_N^{2(2-n)}\rho^{2n-2} - \frac{2(n-1)}{n}\rho_N^{2-n}\rho^n\cos(n\varphi)+o(\rho^n)\right\} \tag{24}$$

At the corner point the isobars have a center point and on the body surface saddle points occur.[8] These saddle points correspond to a minimum in the wall pressure, which, to first order, is given by

$$\frac{p_N}{p_0} = 1-\frac{\gamma}{2}\frac{\Phi_e-\pi}{\Phi_e}M_0^2\rho_N^2 \tag{25}$$

Matching of Local Corner Flow with Two-Dimensional Wedge Flows

To the order indicated in Eq. (22) the expression for the conical potential F contains two free parameters ϵ_n and M_0 which may be used to match the local corner flow with the two-dimensional flow found in the region downstream of the supersonic leading edge. The flow in this region is similar to the flow over the upperside of a wedge and, therefore, will be called the two-dimensional wedge flow. The matching will be performed by requiring continuity of the velocity (in direction and magnitude) on the ray $\rho=\tilde\rho$, the intersection with the body surface of the Mach cone of the two-dimensional wedge flow emanating from the apex of the configuration, Fig. 7. We then obtain

$$F_\rho = (F-\rho F_\rho)\tan\tilde\theta$$

$$\left(1+\frac{\gamma-1}{2}M_{2D}^2\right)\left((1+\rho^2)F_\rho^2-2\rho FF_\rho+F^2\right)=\frac{\gamma-1}{2}M_{2D}^2 \tag{26}$$

at $\varphi=0,\Phi_e$ and $\rho=\tilde\rho$

Here $\tilde\theta$ is the angle between the direction of the two-dimensional wedge flow and the corner line, and M_{2D} is the Mach number of the two-dimensional wedge flow. Substitution of Eq. (22) into Eq. (26) yields

$$n\epsilon_n\tilde\rho^{n-1}+(3n-2)\lambda\epsilon_n^3\tilde\rho^{3n-3} = [1-(n-1)\epsilon_n\tilde\rho^n - 3(n-1)\lambda\epsilon_n^3\tilde\rho^{3n-2}+\mathcal{O}(\tilde\rho^{2n})]\tan\tilde\theta \tag{27}$$

$$M_0^2\left[1+\left(1+\frac{\gamma-1}{2}M_{2D}^2\right)\{n^2\epsilon_n^2\tilde\rho^{2n-2}-2(n-1)\epsilon_n\tilde\rho^n + 2n(3n-2)\lambda\epsilon_n^4\tilde\rho^{4n-4}+o(\rho^{4n-4})\}\right]=M_{2D}^2 \tag{28}$$

which gives ϵ_n, M_0 and as a result also the location of the conical stagnation points and the pressure distribution. It may be seen from Eq. (27) that, for small ϵ_n, ϵ_n and $\tilde\theta$ have the same sign which implies that for compressive wedge angles ($\delta>0$, $\tilde\theta>0$), $\epsilon_n>0$ and for expanding wedge angles ($\delta<0$, $\tilde\theta<0$), $\epsilon_n<0$. If the matching procedure is applied in the case of a symmetrical corner with compressive wedge angles and characterized by $\omega=\pi/2$, $\Lambda=0$, the location of the conical stagnation points on the surfaces is found to depend on the

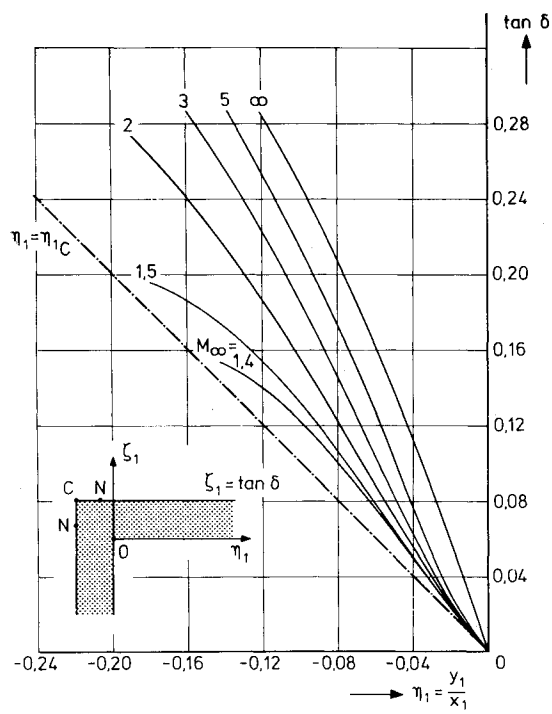

Fig. 8 Position of conical stagnation points as a function of freestream Mach number and wedge angle for a symmetrical configuration with $\Lambda=0$ deg, $\omega=\pi/2$. —·—·— $\eta_I=\eta_{I_C}$, location of corner point; ——— $\eta_I=\eta_{I_N}$, location of nodal point.

parameters δ and M_∞, as shown in Fig. 8. In order to facilitate comparison with results known from the literature, the coordinates η_1, ζ_1 are used in Fig. 8. We remark that the nodal point shifts toward the corner point if compared with the position it would take for the flow around a single wedge, since then $(\eta_1)_N = 0$. Figure 8 seems to indicate that the bifurcation of the starlike node into an oblique saddle point and two nodal points is a higher order effect in δ since, for any finite Mach number M_∞, the lines for $\eta_1 = \eta_{1_C}$ and $\eta_1 = \eta_{1_N}$ seem to approach the origin at equal slope. This effect may be verified by expanding Eq. (27), taking into account that for $\omega = \pi/2$, $\Lambda = 0$, $\tan\tilde{\theta} = \sin\delta$, and using Eq. (13) to obtain the leading term for ρ_N as

$$\rho_N = \tilde{\rho}^{((1-n)/(2-n))}\,\delta^{1/(2-n)} \tag{29}$$

Since on the wedge surface Σ_1 we have $\rho_1 = (\rho - \sin\delta) \times (1 + \rho\sin\delta)^{-1}(\cos\delta)^{-1}$, so that we may write

$$\eta_{1N} = -\delta + \tilde{\rho}^{(1-n)/(2-n)}\,\delta^{1/(2-n)} + \mathcal{O}(\delta)^2, \quad 1 < n < 2$$

$$\eta_{1C} = -\delta + \mathcal{O}(\delta^3) \tag{30}$$

This calculation indicates that in a usual perturbation theory, where δ is the perturbation parameter, such as used in Ref. 6, no bifurcation of the starlike node is likely to appear.

In order to compare the pressure distribution the wedge surfaces with numerical and experimental results we consider the case of $\delta = 10$ deg, $M_\infty = 3$; then $M_{2D} = 2.580$, $\rho_N = 0.0783$. With Eq. (24) we obtain p/p_N which is shown in Fig. 9. The agreement with numerical calculations[5] and experimental results[1] is quite satisfactory, even at greater distance from the corner point. Note that in the numerical calculations entropy gradients are taken into account, whereas the present theory assumes potential flow near the corner, and only a limited number of terms in the expansion are used.

Transition of Bifurcation Mode

Thus far, the use of the first bifurcation mode seems an effective way to describe the flow around a symmetrical external corner with compressive surfaces. As a result two nodal points are always found on the body surface as well as a saddle point at the corner. This general conclusion is unaffected by a change of ω from ($\omega \approx \pi/2$) (the corner type of configuration) to ($\omega \approx \pi$) (the delta wing type). In fact, numerical calculations[5] were performed by Salas for symmetrical configurations ($\delta = 10$ deg, $\Lambda = 20$ deg and 40 deg), $M_\infty = 3$ and values of ω ranging from 90 to 180 deg. According to Salas, these calculations indicate that for higher values of ω no nodal points on the surface are present and the corner point is then a nodal point instead of a saddle point. This would imply that for a certain value of ω a transition from the first bifurcation mode ($k = 2$) to a higher bifurcation mode ($k = 4,6,\ldots$) would take place. However, such a transition also implies the sudden disappearance of the nodal points situated

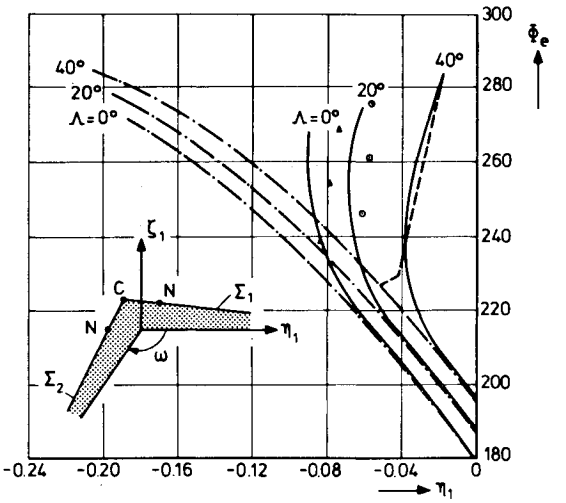

Fig. 10 Position of conical stagnation points on Σ_1 in the first bifurcation mode as a function of the external angle Φ_e, $M_\infty = 3$, $\delta = 10$ deg. Location of corner point —·—·—·. Location of nodal point: ——— present theory; ------- Salas,[6] △ ($\Lambda = 0$ deg) and ○ ($\Lambda = 20$ deg) Salas.[6]

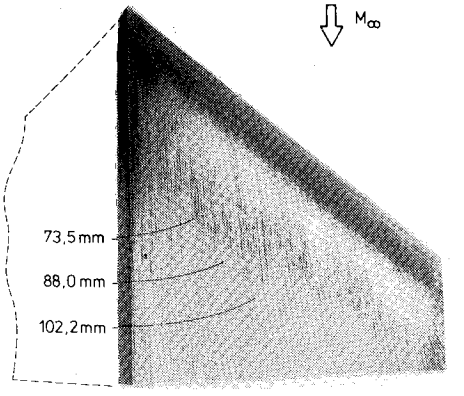

a) Oil flow streaklines, $\alpha = 0$ deg.

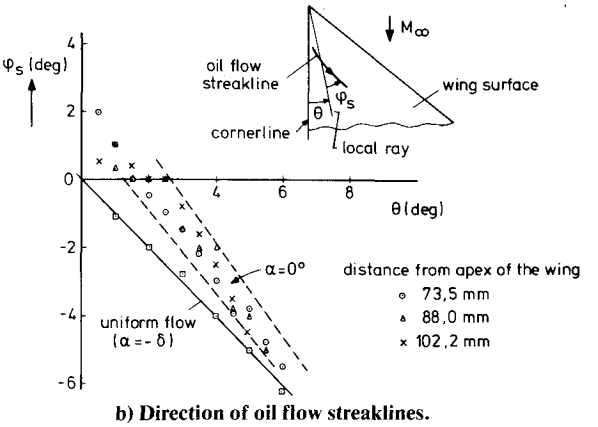

b) Direction of oil flow streaklines.

Fig. 11 Oil flow streaklines on delta wing, $\delta = 10$ deg, $\Lambda = 40$ deg, $\Phi_e = 196.5$ deg, $M_\infty = 3$.

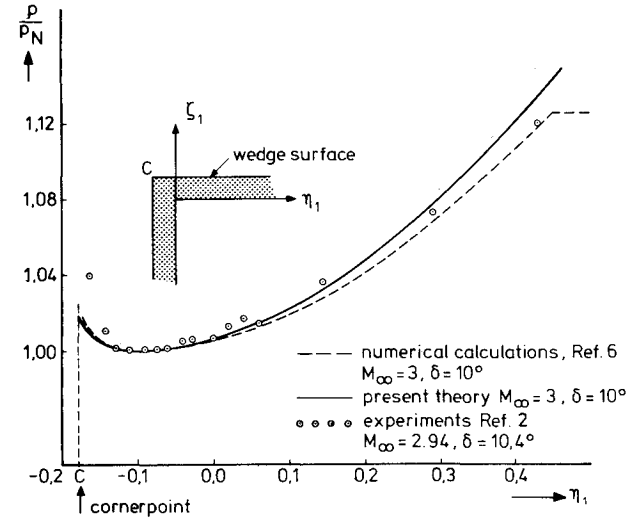

Fig. 9 Pressure distribution along the wedge surface of a symmetrical external corner with $\omega = \pi/2$, $\Lambda = 0$ deg.

away from the corner. This is impossible since such a bifurcation mode does not exist. We further remark that if the nodal points are close to the corner point, they are very difficult to detect in numerical calculations, in contrast to the situation when they can be clearly observed further away from the corner point. In order to show how close the nodal points are to the corner point as ω tends to 180 deg for the configuration of Ref. 5 ($\Lambda = 40$ deg, $\delta = 10$ deg, $M_\infty = 3$) the position of the conical stagnation points was calculated according to the first bifurcation mode; see Fig. 10. In addition, Fig. 10 shows also the results for $\Lambda = 0$ and 20 deg. For these calculations, it appears that for $\Phi_e < \sim 220$ deg the nodal points and the corner point are so close that a numerical detection would be rather unlikely. For $\Phi_e > \sim 220$ deg there is a substantial shift of the nodal points away from the corner point. If we compare the above calculations with the numerical results of Salas[5,9] there is good agreement for $\Lambda = 40$ deg, whereas for $\Lambda = 0$ and 20 deg the agreement is less. As mentioned before, it should be noted that the present results are obtained by using a finite number of terms in a series expansion of potential flow solutions, whereas the numerical calculations use the Euler equations.

Experimental Observations

As experimental results confirming the predicted flow pattern according to the first bifurcation mode have already been reported for the external angle configuration,[2] it is of interest to investigate whether the occurrence of nodal points, distinct from the corner point, can also be observed in experiments with a delta wing configuration, even though these points may lie very close to the corner. For this purpose a flow visualization study has been made on the upper side of a truncated delta wing with a flat lower surface ($\omega = \pi$ rad, $\Lambda = 40$ deg, $\delta = 10$ deg, $\Phi_e = 196.5$ deg) in the 27×28 cm supersonic wind tunnel TST27 at $M_\infty = 3$, $Re = 2.3 \times 10^5$/cm. Although one should be cautious in drawing conclusions on inviscid flow patterns from flow visualization techniques, experiments on external corners[2,4] have shown that the conical nature of the flow is borne out by the oil flow streaklines. The photograph reproduced in Fig. 11a shows the oil streaklines on the upper face of the wing when the incidence α of the plane lower surface (measured in the symmetry plane) is set at 0 deg. From this picture the angle φ_s of the local streamline with the local ray has been carefully measured. The results are collected in Fig. 11b; they do suggest that nodal points may be distinguished in the conical flowfield. The reliability of these results may be judged by comparing them with those obtained for $\alpha = -\delta = -10$ deg, in which case the upper surface is aligned with the flow. Comparing the results for $\alpha = 0$ and -10 deg, a significant shift of the nodal singularity away from the corner is observed.

Acknowledgments

The authors are grateful to J. Boeker for the thorough reading of the manuscript. Thanks are also due N. J. Lam and G. A. F. Bekink for their help in obtaining the flow visualization results.

References

[1] Bakker, P. G., Bannink, W. J., and Reyn, J. W., "Potential Flow near Conical Stagnation Points," *Journal of Fluid Mechanics*, Vol. 105, 1981, pp. 239-260.

[2] Bannink, W. J., "Investigation of the Conical Flow Field About External Axial Corners," *AIAA Journal*, Vol. 22, March 1984, pp. 354-360.

[3] Kutler, P. and Shankar, V., "Computation of the Inviscid Supersonic Flow over External Axial Corners," *Proceedings of the Heat Transfer and Fluid Mechanics Institute*, Davis, Calif., 1976, pp. 356-373.

[4] Salas, M. D. and Daywitt, J., "Structure of the Conical Flow Field About External Axial Corners," *AIAA Journal*, Vol. 17, Jan. 1979, pp. 41-47.

[5] Salas, M. D., "Careful Numerical Study of Flow Fields About Symmetrical External Conical Corners," *AIAA Journal*, Vol. 18, June 1980, pp. 646-651.

[6] Vorob'ev, N. F. and Fedosov, V. P., "Supersonic Flow Around a Dihedral Angle (Conical Case)," Isvestiya Akademii Nauk SSSR, Mekhanika Zhidkostii Gaza, No. 5, 1972, pp. 170-175.

[7] Andronov, A. A., Leontovich, E. A., Gordon, J. J., and Maier, A. G., "Qualitative Theory of Second-Order Dynamic Systems," John Wiley & Sons, New York, 1973.

[8] Bakker, P. G. and Reyn, J. W., "Conical Stagnation Points in the Flow Around an External Corner," Dept. of Aerospace Engineering, Delft University of Technology, the Netherlands, Rept. LR-396, Oct. 1983.

[9] Salas, M. D., private communication, NASA Langley Research Center, Aug. 1983.